ELSEVIER

Journal of Non-Crystalline Solids 235–237 (1998) 605–611

JOURNAL OF NON-CRYSTALLINE SOLIDS

A new separation medium for DNA capillary electrophoresis: self-assembly behavior of Pluronic polyol $E_{99}P_{69}E_{99}$ in 1X TBE buffer

Chunhung Wu, Tianbo Liu, Benjamin Chu *

Department of Chemistry, State University of New York at Stony Brook, New York, NY 11794-3400, USA

Abstract

The unique sol–gel transition property of $E_{99}P_{69}E_{99}$ (with E and P being poly(ethylene oxide) and poly(propylene oxide), respectively), a Pluronic polyol F127, could become a useful separation medium in the miniaturization and automation of capillary electrophoresis (CE). Static light scattering (SLS), dynamic light scattering (DLS), and small-angle X-ray scattering were used to study the solution property and the gel-like structures of F127 in a CE buffer (1X TBE) for DNA separation. F127 in the CE forms core-shell micelles with a closed-association process. The critical micelle concentration (cmc) decreases and the micellar association number increases with increasing temperature. At larger solution concentrations, small-angle X-ray scattering results showed that the gel-like structure formed by close packing of the micelles had a face centered cubic (fcc) lattice. In the gel-like region the association number and also the micellar size were not affected by concentration changes. With F127 solution as a separation medium, CE could be performed successfully with a detection length of only 4 cm for separation of double-stranded DNA (dsDNA) and single-stranded DNA (ssDNA) fragments. © 1998 Published by Elsevier Science B.V. All rights reserved.

1. Introduction

Capillary electrophoresis (CE) with replaceable polymer solution as a sieving medium is an analysis technique for the applications of DNA separation and sequencing [1]. Viscous polymer solutions are usually used to achieve better separation resolution [2]. However, for larger viscosities the solution properties make injection and replenishing of such a separation medium more difficult. Besides, to suppress electroosmotic flow (EOF) and to prevent analyte adsorption, inner wall coatings with compatible polymers are usually necessary. Unfortunately, the stability and the reproducibility of the coatings that usually involve multistep reactions are difficult to control. Therefore, a better separation medium which can provide the better separation resolution but is also easy to handle, can be very useful.

In this paper, we present some studies on the self-assembly behavior of F127 in a DNA buffer, its gel-like structure at some polymer concentrations, and the performance as a separation medium in CE for DNA separation. B.C. wishes to dedicate this work in honor of Professor E.W. Fischer, whose pioneering and definitive studies on polymers using laser light scattering (LLS) and small-angle X-ray scattering give inspiration to

* Corresponding author. Tel.: 1 516 6327928; fax: 1 516 6327960; e-mail: bchu@notes.cc.sunysb.edu.

0022-3093/98/$19.00 © 1998 Published by Elsevier Science B.V. All rights reserved.
PII: S0022-3093(98)00570-5

the present investigation, aiming to expand the applications of polymer physics to a bioanalytical tool: capillary electrophoresis.

2. Experimental procedures

2.1. Materials

F127 solutions: F127 ($E_{99}P_{69}E_{99}$) solutions were prepared by mixing polymers (a gift from the BASF Corporation, Parsippany, NJ) with 1X TBE buffer (89 mM tris(hydroxymethyl)aminomethane, 89 mM boric acid, and 2 mM EDTA in deionized water), to desired concentrations. The mixture was stirred in an ice bath for at least 1 h and then stored in a refrigerator at 4°C for a few days before use. The F127 solutions for LLS experiments were prepared by diluting a stock solution of 100 mg/mL. Dust-free solutions were obtained by filtering the diluted solutions through Millipore sterile membrane filters (0.1 μm pore size) into 17-mm-o.d. cylindrical light-scattering cells, which had been rinsed with distilled acetone.

DNA samples: ϕX174 DNA-Hae III digest was purchased (New England Biolabs, Inc.). This dsDNA sample was diluted to 10 μg/mL by using the 1X TE buffer (10 mM Tris · HCl + 1 mM EDTA). The oligonucleotide sizing marker was the product of Pharmacia Biotech. The ssDNA sample was diluted ten times with deionized water from stock solution to a concentration of 1.6 μg/mL. Prior to sample injection, the ssDNA sample was heated at 90°C for two minutes.

2.2. Capillary electrophoresis

A 6-cm long fused silica capillary (Polymicro Technologies) with ID/OD = 98 μm/364 μm was flushed with 1 mL of 1 N HCl over a period of about 10 min. A detection window of 2-mm width was opened at 4 cm from the cathodic end by stripping the polyimide coating off with a razor blade. The running buffer is 1X TBE and 3 μg/mL ethidium bromide. The DNA sample was electrokinetically injected into the capillary tubing at an electric field strength of 300 V/cm for 5 s. The runtime electric field strengths were 200 V/cm for dsDNA and 150 V/cm for ssDNA. The CE instrument has been described elsewhere [3].

2.3. Laser light scattering

A laboratory-built LLS spectrometer [4] operating at a wavelength of 514.5 nm with an output power of about 600 mW was used to perform static light scattering (SLS) and dynamic light scattering (DLS) measurements at a scattering angle of 90° over a range of temperatures from 20°C to 42°C. The intensity correlation function was measured by using a Brookhaven BI-2030 digital correlator.

2.4. Small-angle X-ray scattering (SAXS) experiments

SAXS experiments were performed at the X3A2 SUNY Beam Line, National Synchrotron Light Source (NSLS) at Brookhaven National Laboratory (BNL), using a laser-aided pre-aligned pinhole collimator [5]. The incident beam wavelength (λ) was tuned at 0.154 nm. Fuji imaging plates were used as the detection system. The sample-to-detector distance was 1085 mm.

3. Results

3.1. LLS study on the dilute solution property of F127

The critical micelle concentration (cmc) is defined as the concentration at which the LLS intensity departs from the baseline intensity contributed only by unimers. Fig. 1 shows two representative plots of SLS results for the determination of the cmc. The cmc value was estimated by the intersection of the two linear regression lines with cmc = 0.4 mg/mL at 30°C and 52.0 mg/mL at 20°C. The relative excess scattered intensity I_{ex} was calculated by $(I - I_0)/I_{BZ}$, where I, I_0, and I_{BZ} are the scattered intensity of polymer solution, 1X TBE buffer, and benzene, respectively. The dashed line in Fig. 1(a) represents the I_{ex} value of unimers in an ideal solution, where the second virial coefficient $A_2 = 0$. The cmc values estimated

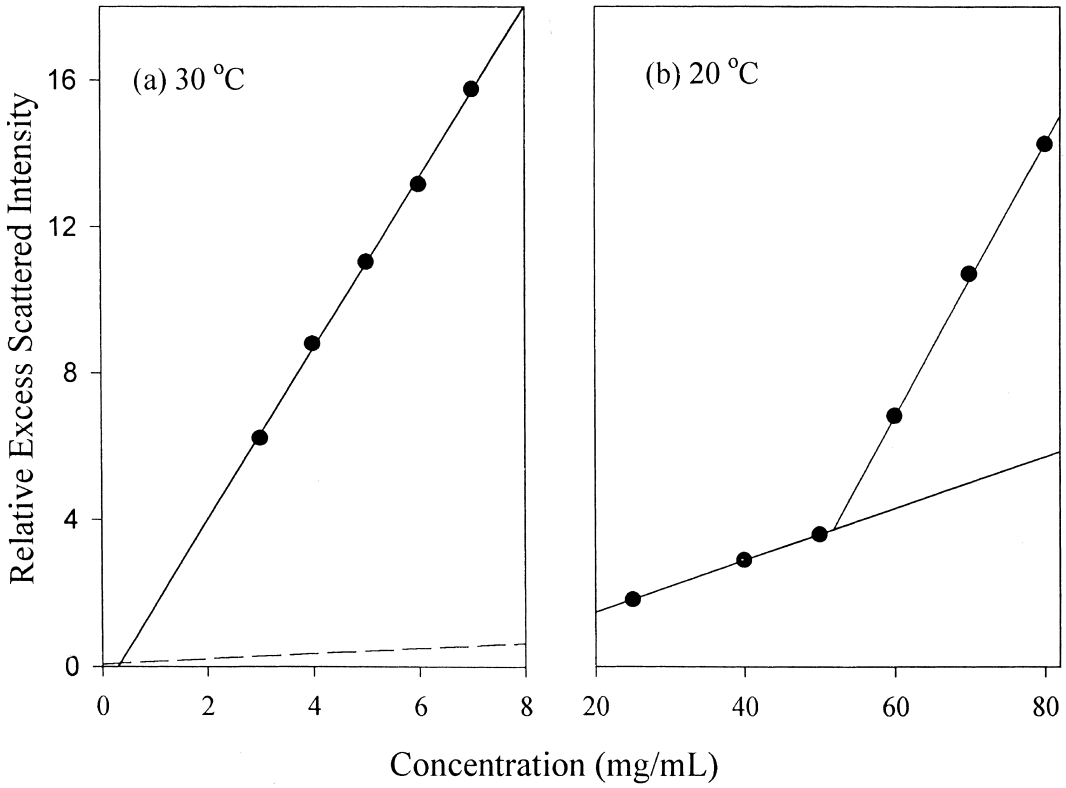

Fig. 1. Plots of relative excess scattered intensity at $\theta = 90°$ versus concentration of $E_{99}P_{69}E_{99}$ in 1X TBE buffer solution at (a) 30°C and (b) 20°C.

from SLS are 6.1, 0.03 and 0.003 mg/mL at 25°C, 35°C and 40°C, respectively.

To calculate the micellar association number, we use the equation

$$HC_{cmc}/R_{mic,90} = 1/M_w + 2A_2C_{cmc}, \quad (1)$$

where $H(=4\pi n_0^2(dn/dc)^2/N_A\lambda^4)$ is an optical constant with n_0 being the refractive index of solvent; dn/dc, the refractive index increment; N_A, Avogadro's constant; λ, the laser light wavelength (514.5 nm); $R_{mic,90}(= R_{BZ,90}((I - I_{cmc})/I_{BZ})\ (n^2/\ n_{BZ}^2))$ the Rayleigh ratio of micelle at 90° with I_{cmc}, C_{cmc}, n, and n_{BZ} being the scattered intensity at cmc, the polymer concentration at cmc, the refractive index of solution and of benzene, respectively; M_w, the weight-average molecular weight; and A_2, the second virial coefficient. From the plot of $HC_{cmc}/R_{mic,90}$ versus C_{cmc}, the micellar weight-average molecular weight at different temperatures can be estimated by extrapolating C_{cmc} to zero. The association numbers (n_w) thus derived are plotted versus temperature in Fig. 2. The solid line is the linear regression of the data points between 25°C and 40°C. The dotted line is an extension of the solid line and is used to indicate that the data point at 20°C deviates from the linear relationship.

DLS measures the intensity–intensity time correlation function $G^{(2)}(\tau)$, with τ being the delay time. A Laplace inversion (we used the CONTIN method [6] for the data analysis) of $G^{(2)}(\tau)$ yields the normalized characteristic linewidth distribution function $G(\Gamma)$. The characteristic linewidth Γ can be related to the translational diffusion coefficient D by $D = \Gamma/q^2$, with q being the magnitude of the momentum transfer vector. With the Stokes–Einstein relation, which applies in the dilute solution region, the hydrodynamic radius has the form

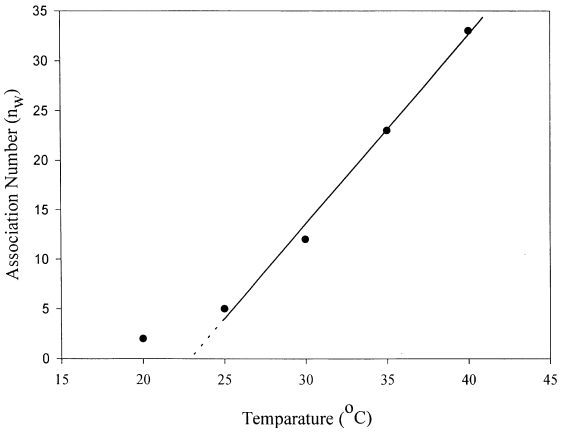

Fig. 2. Plot of the association number (n_w) of solution in 1X TBE buffer versus temperature.

$$R_h = k_B T/(6\pi\eta D) \quad (2)$$

where k_B is the Boltzmann constant and η is the solvent viscosity at temperature T, we can determine the apparent hydrodynamic radius, $R_{h,app}$, where we have neglected the intermolecular interactions. Fig. 3 shows the effects of concentration and temperature on the $R_{h,app}$ values of dilute $E_{99}P_{69}E_{99}$ solution in 1X TBE buffer. At 25°C and 7 mg/mL, which is slightly higher than the cmc of 6.1 mg/mL, micelles coexist with unimers. By increasing the concentration to 15 mg/mL, the micellar peak dominates; however, the average $R_{h,app}$ remains the same. By increasing the temperature to 42°C, the dynamic equilibrium between unimers and micelles is shifted in favor of micelles. Therefore, only the micellar peak is observed in Fig. 3(c). The $R_{h,app}$ of micelles at 42°C is only slightly larger than that at 25°C even though n_w has grown by a factor of more than 6, as shown in Fig. 2.

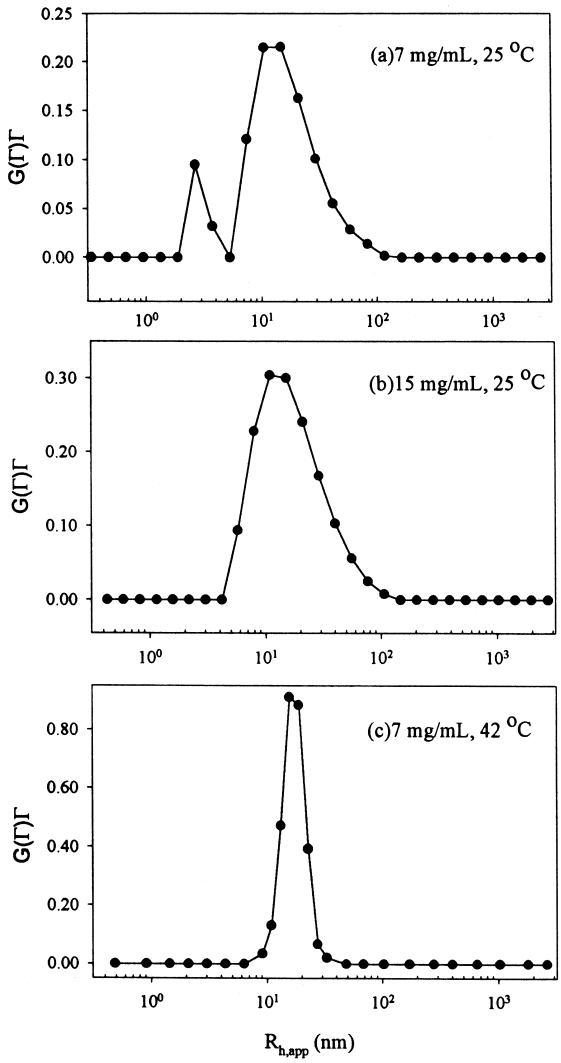

Fig. 3. Plots of intensity contribution function $\Gamma G(\Gamma)$ versus apparent hydrodynamic radius $R_{h,app}$ of $E_{99}P_{69}E_{99}$ solution in 1X TBE buffer under three different conditions as indicated in the figure. The CONTIN method [6] was used for the data analysis. Lines are drawn as guides for the eye.

3.2. SAXS study on F127 gel structure

Fig. 4 shows the SAXS images of 21.2 (wt/v)% and 28.0 (wt/v)% $E_{99}P_{69}E_{99}$ in 1X TBE buffer solutions. The corresponding circular integration profiles are shown in Fig. 5. The results are distinct from the usual broad and homogenous scattering rings obtained from small angle neutron scattering (SANS) [8]. Instead, bright scattering dots which appeared in several concentric rings can clearly be visualized in the SAXS images. The integration profiles in Fig. 5 shows seven well resolved peaks with the ratio of relative peak positions being 1: $(4/3)^{1/2}$: $(8/3)^{1/2}$: $(11/3)^{1/2}$: 2: $(16/3)^{1/2}$: $(19/3)^{1/2}$. Based on the Bragg diffraction peaks from SAXS we are able to determine the $E_{99}P_{69}E_{99}$ gel structure as

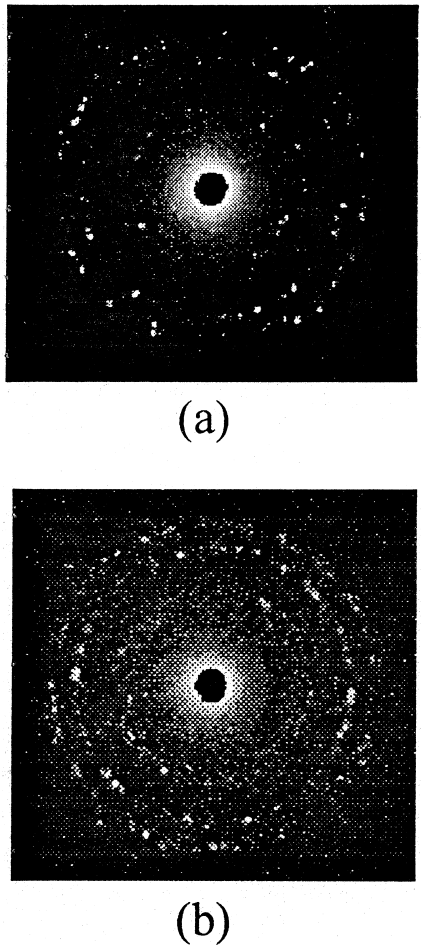

Fig. 4. SAXS images of (a) 21.2 (wt/v)% (cited from Ref. [7], Fig. 13(b) for comparison with Fig. 4(b)) and (b) 28.0 (wt/v)% $E_{99}P_{69}E_{99}$ in 1X TBE buffer. The corresponding SAXS intensity profiles are shown in Fig. 5.

a face centered cubic (fcc) latice. The corresponding diffraction planes can also be indexed as (1 1 1), (2 0 0), (2 2 0), (3 1 1), (2 2 2), (4 0 0), and (3 1 3). From the lattice structure and size, we can further calculate the micellar association number n_w for the $E_{99}P_{69}E_{99}$ gel. For the fcc crystal structure, the number density ρ can be described as

$$\rho = 4/a^3 = CN_A/(n_w M_{wt}), \tag{3}$$

where a is the dimension of a unit cell and can be calculated from the first order peak [8], C (wt/v) is the polymer solution concentration and M_{wt} is the

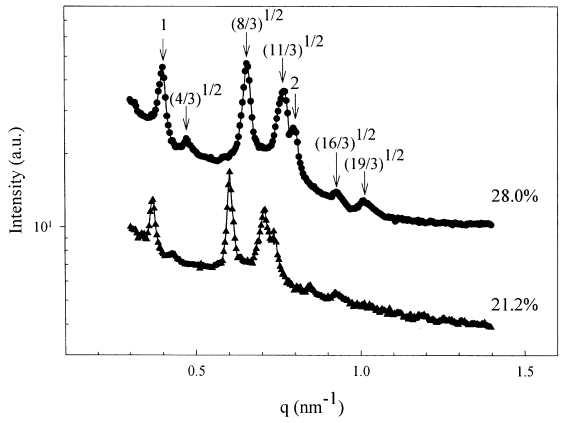

Fig. 5. SAXS intensity profiles of 21.2 (wt/v)% and 28.0 (wt/v)% $E_{99}P_{69}E_{99}$ in 1X TBE buffer at 25°C. The arrows indicate the peak positions. The numbers represent the ratio of the peak position relative to the first order peak. The corresponding SAXS images are shown in Fig. 4.

molecular weight of the polymer. From Eq. (3) we can derive n_w as

$$n_w = CN_A a^3/(4M_{wt}). \tag{4}$$

By assuming that the micellar core consists of only P blocks and that all P blocks reside in the micellar core, we can estimate the core radius, R_c, by using n_w and the following relation

$$(4/3)\pi R_c^3 = n_w M_{wt,PPO}/(N_A \rho_{PPO}), \tag{5}$$

where $M_{wt,PPO}$ is the molecular weight of the PPO block, and ρ_{PPO} is the density of PPO. Here we have used PPO ≡ P. The calculated n_w and R_c are, respectively, 65 and 4.6 nm for 21.2% $E_{99}P_{69}E_{99}$ gel and 66 and 4.6 nm for 28.8% $E_{99}P_{69}E_{99}$ gel at 25°C.

3.3. Application of $E_{99}P_{69}E_{99}$ solution to capillary electrophoresis

The resolution performances of both ssDNA and dsDNA separations in CE by using the $E_{99}P_{69}E_{99}$ solution in 1X TBE buffer are demonstrated in Fig. 6. All eleven dsDNA fragments were resolved in less than 18 min. The peak assignments are in accordance with the integrated peak areas. In Fig. 6(b), the 20-base peak was used as an internal standard to assign the peak positions.

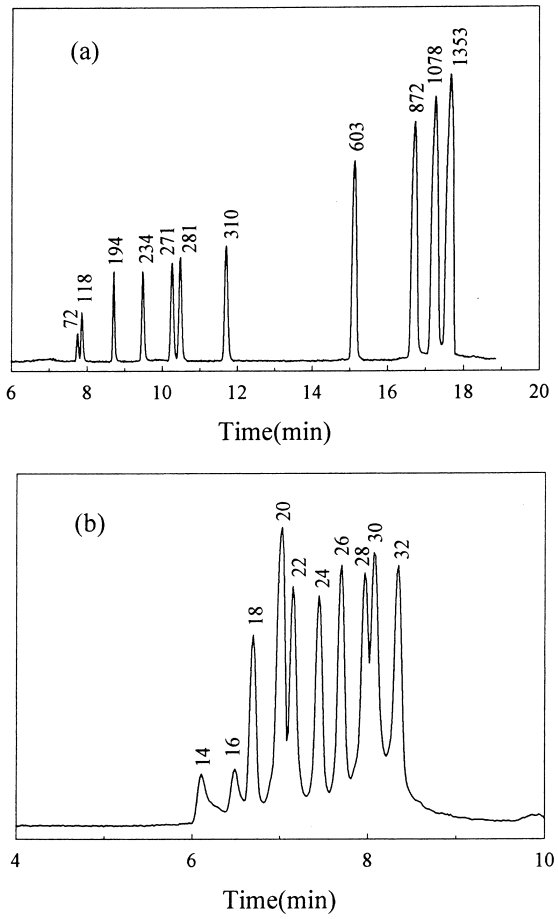

Fig. 6. Electropherograms of (a) ϕX174 DNA-Hae III digest and (b) oligonucleotide sizing markers obtained by using 21.2 (wt/v)% $E_{99}P_{69}E_{99}$ gel at room temperature. Peak assignments are as indicated in the plots.

4. Discussion

4.1. Dilute solution property of $E_{99}P_{69}E_{99}$ in TBE buffer

In the dilute solution region, the property of $E_{99}P_{69}E_{99}$ in TBE buffer is similar to that in an aqueous solution. Increasing the temperature to room temperatures increases the hydrophobicity of the P block and thus induces the micellar formation. The n_w increases linearly with increasing temperature from 25°C to 42°C. This phenomenon was commonly found in the dilute solution regime of Pluronic polyols. There was an exception at 20°C where $n_w \cong 2$, which corresponded more closely to a molecular associate rather than a core-shell micelle. At 25°C, the smaller n_w suggests that the P blocks form a core which could contain a substantial amount of buffer with the core having a somewhat porous structure. At 42°C micelles became more dense both in the core and in the corona to accommodate a substantial increase in n_w. It is also noted that the micellar size distribution became narrower with increasing temperature as shown schematically in Fig. 3(a) and (c). Similar phenomena have been reported in other Pluronic block copolymer systems [9].

4.2. $E_{99}P_{69}E_{99}$ gel structure

At larger polymer concentrations the Bragg diffraction peaks shift to a larger q range. From the results of n_w calculation, we visualize, schematically, that the micelles have the same overall size at larger polymer concentrations. An increase in the micelle number density results in a larger degree of overlap between the micellar coronas of the E blocks. Thus, a decrease in the inter-micellar distance is observed by a corresponding shift in the diffraction peaks to larger qs.

4.3. DNA separation performance

The viscosity adjustable $E_{99}P_{69}E_{99}$ solution can be utilized to form a gel-like structure with sieving ability and can also serve as a dynamic coating material [10,11], thereby effectively suppressing the electroosmotic flow induced by the ionization of the silanol group on the quartz capillary inner wall. When applied to CE as a separation medium, $E_{99}P_{69}E_{99}$ block copolymer can provide the advantages of better separation resolution, easy injection and replacement of the triblock copolymer solution, and convenient capillary column treatment.

5. Conclusions

At low concentration and low temperature, the 1X TBE buffer is a good solvent for both P and E blocks. Micellar formation can be induced by in-

creasing the temperature or the polymer concentration. In the solution region where micelles dominate, micellar $R_{h,app}$ remains relatively constant although the association number increases with increasing temperature. At larger polymer concentrations, micelles tend to pack into some quasi-crystalline structures with relatively well structured P centers. By using the SAXS results, we are able to conclusively determine the gel structure to have a fcc lattice. $E_{99}P_{69}E_{99}$ behaves similarly in water and in 1X TBE buffer. In the gel-like region the association number and also the micellar size are less sensitive to concentration changes. Larger concentration results only in closer micellar packing. Fast and excellent ds and ssDNA electrophoretic separations can be achieved by using a 4-cm detection length capillary filled with 21.2% $E_{99}P_{69}E_{99}$ solution at 25°C.

Acknowledgements

B.C. gratefully acknowledges support of this research by the National Human Genome Research Institute (NIH 1R0 1HG0138601), the National Science Foundation (DMR-9612386), and the US Department of Energy (DOE DEFG0286ER452 37.013). The SUNY X3 beamline at NSLS is supported by the Division of Basic Energy Sciences of the US Department of Energy (DE-FG02-86ER45231). Research carried out in part at the National Synchrotron Light Source at Brookhaven National Laboratory which is supported by the US Department of Energy, Division of Materials Sciences and Division of Chemical Sciences.

References

[1] M.A. Adams, C. Fields, J.C. Venter, Automated DNA Sequencing and Analysis, Academic Press, London, 1994.
[2] P.D. Grossman, D.S. Soane, Biopolymers 31 (1991) 1221.
[3] C. Wu, M.A. Quesada, D.K. Schneider, R. Farinato, F.W. Studier, B. Chu, Electrophoresis 17 (1996) 1103.
[4] Z.L. Wang, B. Chu, Q.-W. Wang, L. Fetters, New Trends in Physics and Physical Chemistry of Polymers, Plenum, New York, 1989.
[5] B. Chu, P.J. Harney, Y. Li, K. Linliu, F. Yeh, B.S. Hsiao, Rev. Sci. Instrum. 65 (1994) 597.
[6] S.W. Provencher, Biophys. J. 16 (1976) 29; J, Chem. Phys. 64 (1976) 2772.
[7] C. Wu, T. Liu, B. Chu, D.K. Schneider, V. Graziano, Macromolecules 30 (1997) 4574.
[8] R.K. Prud'homme, G. Wu, D.K. Schneider, Langmuir 12 (1996) 4651.
[9] P. Alexandridis, T. Nivaggioli, T.A. Hatton, Langmuir 11 (1995) 1468.
[10] C. Wu, T. Liu, B. Chu, Electrophoresis 19 (1998) 231.
[11] R.L. Rill, B.R. Locke, Y. Liu, D.H. Van Winkle, Proc. Nat. Acad. USA 95 (1998) 1534.